Macromolecular Research

Article

DOI 10.1007/s13233-022-0090-0

www.springer.com/13233 pISSN 1598-5032 eISSN 2092-7673

Biomimetic Calcium Phosphate Coated Macro-Microporous Poly(ε-caprolactone)/Silk Fibroin (PCL/SF) Scaffold for Bone Tissue Engineering

Nomin-Erdene Tumursukh[1]
Joo Hee Choi[1]
Jin Sol Seo[1]
Youngeun Song[1]
Gayeong Jeon[1]
Na Eun Kim[1]
Jeong Eun Song[1]
Gilson Khang*[,1,2,3]

[1] Department of Bionanotechnology and Bio-Convergence Engineering, Jeonbuk National University, 567 Baekje-daero, Deokjin-gu, Jeonju-si, Jeonbuk 54896, Korea
[2] Department of PolymerNano Science & Technology and Polymer Materials Fusion Research Center, Jeonbuk National University, 567 Baekje-daero, Deokjin-gu, Jeonju-si, Jeonbuk 54896, Korea
[3] Department of Orthopaedic & Traumatology, Airlangga University, Jl. Airlangga No.4 - 6, Airlangga, Kec. Gubeng, Kota SBY, Jawa Timur 60115, Indonesia

Received January 10, 2022 / Revised May 2, 2022 / Accepted June 24, 2022

Abstract: Because of an aging population and social development, tissue engineering techniques have been widely studied and used for patient treatment. To improve bone regeneration and overcome disadvantages, suitable biomaterials have to be chosen. Polycaprolactone (PCL) is extensively used in bone tissue engineering, known for its excellent mechanical properties, high crystallinity, toughness, and biocompatibility. In addition, porous PCL can induce bone ingrowth into its macropores and can be used for the repair and regeneration of the bone. However, PCL has limited cell affinity primarily owing to the lack of cell recognition sites due to its hydrophobic surface. To compensate drawbacks of PCL scaffolds, silk fibroin (SF), nonsolvent and thermal-induced phase separation (N-TIPS), and salt-leaching were utilized in this study. Additionally, to overcome the disadvantage that the polymeric scaffold may be insignificant for osteoinduction, PCL/SF scaffolds were coated with calcium phosphate (CaP) (c-PCL/SF). Physicochemical properties, biological activity, and mechanical characters were analyzed to confirm applicability in bone tissue engineering. Also, in vitro study was performed with viability test, morphology study, proliferation test, and gene expression evaluation. The mechanical property of the c-PCL/SF scaffold was improved when compared to the coated PCL scaffold (c-PCL), and the bioactivity of the c-PCL/SF showed a high amount of apatite formation. Also, bone marrow stem cells (BMSC) cultured in c-PCL/SF scaffolds showed enhanced viability and bone-specific gene expression than the BMSC cultured in c-PCL. Overall, the c-PCL/SF scaffolds were compatible material to apply in bone tissue engineering biomaterial.

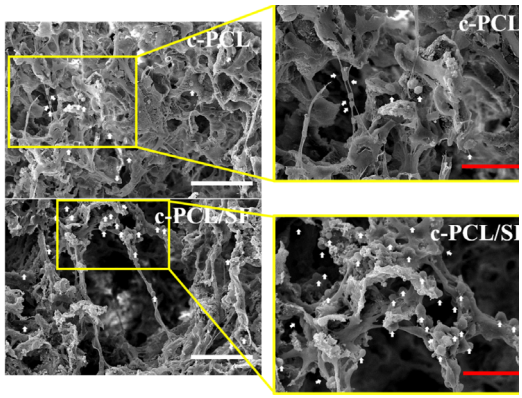

Keywords: scaffold, bone tissue engineering, polycaprolactone, silk fibroin, porous structure.

1. Introduction

Because of an aging population and social development, bone defects and functional disorders that occur from trauma, infection, and tumors have turned into a clinical problem and socio-economical need recently.[1,2] Tissue engineering techniques using cells, drugs, biological agents, scaffolds, etc. have been widely studied and used for patient treatment. The main challenge in tissue engineering is choosing suitable biomaterials that improve bone regeneration and overcome disadvantages.[3,4] To design biomaterials for bone tissue engineering, chemical, physicochemical structural properties, fabrication process, and microenvironment for cell growth have to be considered.[1,5]

Polycaprolactone (PCL) is a semi-crystalline polyester approved by the US Food and Drug Administration (FDA). It is widely used in bone tissue engineering due to advantages such as excellent biocompatibility, high crystallinity, great mechanical strength, and remarkable toughness.[6] PCL has a longer degradation time and an erosion rate among all polyesters.[7] It is due to the presence of five hydrophobic -CH_2 groups in repeating units.[8] However, because of the hydrophobic surface of the PCL, it has poor cell adhesion, migration, proliferation, and differentiation.[9] Therefore, it is important to improve the microenvironment of PCL with a biomaterial that can enhance integrin-ligand interaction or modify the PCL backbone with cell surface receptors.[10]

Herein, silk fibroin (SF) and calcium phosphate (CaP) coating were applied to compensate for the shortcoming of the PCL scaffold. Also, the macro- and microporous structure of the PCL scaffold was fabricated by salt leaching; creation of pores through washing out salt particles from the scaffolds, gas foaming; the reaction of sodium hydrogen carbonate ($NaHCO_3$) with

Acknowledgment: This research was supported by the bilateral cooperation Program of the National Research Foundation of Korea (NRF) funded by the Ministry of Science, ICT & Future Planning (2019K2A9A1A06098563).

***Corresponding Author:** Gilson Khang (gskhang@jbnu.ac.kr)

acid and forms carbon dioxide gas, N-TIPS; a combination of two methods such as thermally induced phase separation (TIPS) which is based on the change in temperature and non-solvent induced phase separation (NIPS) which is based on an interaction between polymer, solvent and non-solvent methods; to fabricate scaffolds under controllable and scalable conditions.[11-14]

SF has been widely used for biomedical applications because of its easy processing among natural polymers.[15] Also, it has excellent biocompatibility and improves the microenvironment of the scaffolds by providing cell attachment sites.[6] It was suspected that the hydrophilicity of PCL may be improved through the hydrophilic sequence of the light chain of SF.[16] Various techniques for improving osteoconductivity, such as calcium phosphate coating, have been utilized. Common methods for coating calcium phosphate on the surface of biomaterials include electrostatic or plasma spraying, coating through sol-gel phase shift and magnetron sputtering. To accelerate osteoconductivity and osteoinductivity of PCL-based scaffolds, the biomimetic coating with simulated body fluid (SBF) solution was performed to form HA crystals.[17] Biomineralization in osteoblasts is important for bone tissue engineering.[18,19] One of the main components for forming bone and teeth is hydroxyapatite (HA) which natural form is calcium phosphate (CaP). The CaP increases osteoconductivity and osteoinductivity for bone ingrowth.[20] Also, CaP-coated scaffolds release calcium ions and the ions can improve protein adhesion, attachment, and activation of osteoblasts on bone regeneration.[21] The PCL scaffold which was coated with calcium phosphate showed improved cell proliferation and ALP activity compared to the non-coated scaffold, but there was a slight difference in cell adhesion. PCL/SF scaffolds showed better mechanical properties, cell adhesion and differentiation compared to only PCL scaffolds. Therefore, it is possible to make a scaffold that can further upgrade mechanical strength, osteoconductivity and osteoinductivity, and cell adhesion, proliferation and differentiation by coating the PCL/SF scaffold with calcium phosphate.

In this work, we will compare and confirm the effects of biomimetic coating of PCL which is a synthetic polymer typically used in bone tissue and SF which is a natural polymer, on bone regeneration and bone induction of BMSCs. The biomimetic porous PCL/SF scaffold was characterized with XRD, FE-SEM, and EDS analysis to confirm enhanced biological activity of PCL/SF.[22,23] The physicochemical properties and mechanical characters of the fabricated scaffolds were studied with mass swelling, weight loss, porosity, and compression test. Finally, to examine biocompatibility and osteogenesis of the scaffolds, live/dead assay, MTT assay, dsDNA content analysis, real-time polymerase chain reaction (RT-PCR) were carried out.

2. Experimental

2.1. Preparation of silk fibroin (SF)

10 g of small pieces of silkworm cocoons from *bombyx mori* (Kyebong Farm, Cheongyang, Korea) were boiled in 0.02 M sodium carbonate (Na_2CO_3; Showa, Japan) for 30 min to remove sericin. The degummed silk was washed with distilled water and was dried in a 60 ℃ oven. Dried silk was dissolved in 9.3 M lithium bromide (LiBr; Kanto chem., Japan) at a 60 ℃ oven for 4 hrs. The silk solution was dialyzed in distilled water using a dialysis tube (Snake Skin® Dialysis Tubing 3,500 MWCO (molecular weight cut-off), Thermo SCIENCE, USA) for 72 hrs to remove LiBr. The final concentration of the SF was 7% (w/v) and diluted to 1% (w/v) to fabricate the scaffolds.

2.2. Fabrication of poly(ε-caprolactone) (PCL) scaffolds

10% (w/v) poly(ε-caprolactone) (PCL; Sigma-Aldrich, USA) was dissolved in 1,4-dioxane (Sigma-Aldrich, USA) and 1% (w/v) SF was added to the PCL solution to make a final concentration of 9.9% PCL and 0.1% SF. Also, distilled water was added to the PCL solution to fabricate the control scaffold. Sodium chloride (355-425 μm, NaCl, Showa, Japan) and sodium bicarbonate (45-75 μm, $NaHCO_3$, Sigma-Aldrich, USA) were added in with an amount of 13 g and 7 g, respectively in 10 mL of PCL and PCL/SF solution. Then, the composite was poured into a silicone mold with a diameter of 10 mm and a height of 5 mm and transferred to -20 ℃ for 4-5 hrs. The composite was immersed into 100 mL pre-cooled ethanol for 2 days to extract dioxane. The ethanol was exchanged every 8 hrs. Furthermore, the samples were treated with pH 4 hydrochloric acid (HCl; Samchun, South Korea) aqueous solution for 8 hrs to induce $NaHCO_3$ gas foaming. Then the scaffolds were immersed into distilled water for 3 days to remove NaCl. The distilled water was replaced every 8 hrs. The scaffolds were sequentially stored at 4 ℃, -20 ℃, and deep freezer (-80 ℃) for 1 day each and then freeze-dried for 2 days to completely remove water.

2.3. Biomimetic calcium phosphate coating

To activate the surface of the scaffolds, the prepared scaffolds were immersed in 70% ethanol (Sigma-Aldrich, USA) and were placed under a vacuum for 10 min. Then the scaffolds were treated with pre-warmed 2 M sodium hydroxide (NaOH; Sigma-Aldrich, USA) aqueous solution and placed under vacuum for 5 min. After the treatment, the scaffolds were rinsed 3 times with distilled water. A simulated body fluid (SBF) was prepared by mixing sodium chloride (NaCl; Junsei, Japan), potassium chloride (KCl; Sigma Aldrich, Germany), calcium chloride dihydrate ($CaCl_2 \cdot 2H_2O$; Sigma Aldrich, Germany), magnesium chloride hexahydrate ($MgCl_2 \cdot 6H_2O$; Sigma Aldrich, Germany), disodium phosphate (Na_2HPO_4; Sigma Aldrich, Germany), and sodium hydroxycarbonate ($NaHCO_3$; Shinyo pure chemicals co., LTD, Japan).[29] The detailed recipe of the SBF solution is stated in Table 1. The solution was filtered through a 0.22 μm filter (Millipore, USA) and 20 scaffolds were immersed into 35 mL of the SBF solution. The scaffolds were incubated at 37 ℃ for 2 hrs and the solution was replaced every 30 min. After the coating process, they were rinsed in distilled water twice. For the post-treatment, the scaffolds were treated with 0.5 M NaOH and stored at a 37 ℃ oven for 30 min. Then, the scaffolds were rinsed with distilled water 3 times and stored at RT to remove water.

Table 1. Preparation of 10× concentrated SBF solution (1 L)

Reagent		Order	Amount (g)
Sodium chloride	NaCl	1	29.21
Potassium chloride	KCl	2	0.18
Calcium chloride dihydrate	$CaCl_2$*$2H_2O$	3	1.84
Magnesium chloride hexahydrate	$MgCl_2$*$6H_2O$	4	0.51
Disodium phosphate	Na_2HPO_4	5	0.71
Sodium hydroxycarbonate	$NaHCO_3$	6	0.42

2.4. Characterizations of the scaffolds

2.4.1. Bio-LV scanning electron microscope (SEM)

The morphology of the coated PCL (c-PCL) and coated PCL/SF (c-PCL/SF) scaffolds were observed under a Bio-LV scanning electron microscope (SEM, Japan, HITACHI) after gold sputtering twice.

2.4.2. Coating characterization

Field emission scanning electron microscope (FESEM, SUPRA 40VP, Carl Zeiss, Germany) was used to characterize the formation of HA on the surface of the scaffolds and elemental compositions were analyzed by energy-dispersive X-ray spectroscopy (EDS, EDS detector, SUPRA 40VP, Carl Zeiss, Germany). The scaffolds were coated with platinum for the observation.

2.4.3. Physicochemical analysis

The scaffolds were incubated in PBS for 24 hrs in a 37 ℃ incubator. The weight of the wet samples was measured (W_w) and was frozen in a deep freezer overnight. Then the samples were lyophilized for 48 hrs. The weight of the lyophilized specimens was measured (W_d). The mass swelling ratio was calculated using the equation of (1). For the weight loss (%), the weight of the scaffolds was measured after immersing the scaffolds in PBS for 24 hrs in a 37 ℃ incubator. (W_f). At the specific time point, the weight of the scaffolds was recorded (W_s). The weight loss (%) was calculated using the equation of (2). The weight loss was analyzed for 28 days and PBS was changed every 3 days. For the porosity characterization, the diameter and thickness of the scaffolds were measured, and immersed in 1 mL ethanol (V_1) was added to each scaffold. The scaffolds were incubated in a 37 ℃ incubator for 24 hrs. After incubation, the scaffolds were removed and the volume of the remaining solution (V_3) was measured by disposable syringe. The volume V_2 was calculated by using an quation of (3) and the porosity was calculated using the Eq. (4).

$$\text{Mass swelling} = \frac{W_w}{W_d} \tag{1}$$

$$\text{Weight loss (\%)} = \frac{W_f - W_s}{W_f} \times 100(\%) \tag{2}$$

$$V_2 = \pi r^2 h + V_1 \tag{3}$$

$$\text{Porosity (\%)} = \frac{V_1 - V_3}{V_2 - V_3} \times 100(\%) \tag{4}$$

2.4.4. Compressive modulus evaluation

The compressive strength of the scaffolds was evaluated by using a Texture Analyzer (TMS-pro, Sterling, USA). Before the evaluation of compressive strength, the diameter and thickness of the scaffolds were measured with a caliper (Mitutoyo, South Korea). The scaffolds were compressed at the speed of 2 mm/min with a load cell of 10 N.

2.5. *In vitro* study

2.5.1. Isolation and culture of bone marrow stem cells from the rabbit model

The bone marrow of the rabbit was harvested from a New Zealand white rabbit (6 weeks old, Hanil, South Korea) with the guidelines and approval of Chonbuk National University Animal Care Committee, Jeonju, Republic of Korea (CBNU 2016-50). The isolated femurs and tibias were washed with phosphate-buffered saline (PBS; Gibco, USA) 3 times and with 1.5% of Penicillin/Streptomycin (PS; Gibco, Big Cabin, OK, USA) 2 times. The end part of the bone was cut, then bone marrow was isolated by tapping. Bone marrow stem cells from a rabbit model (rBMSCs) were cultured in an Alpha Modified Eagle Medium (Advanced DMEM; Gibco, USA) supplemented with 20% of bovine serum (FBS; Gibco, USA) and 1.2% of PS. rBMSCs were cultured in standard cell culture conditions (5% of CO_2, 37 ℃) incubator and the medium was changed every 3 days.

2.5.2. Preparation of cell-laden scaffolds

Before seeding cells on the scaffolds, all the prepared scaffolds were sterilized under a clean bench with 70% ethanol for 15 min and were rinsed 3 times with PBS for 15 min under UV light. Trypsin (Gibco, USA) was used to dissociate the cultured rBMSCs. Then rBMSCs were seeded on the scaffolds with a cell density of 1×10^5 cells/scaffolds. The cell-laden scaffolds were cultured in the Advanced DMEM cell culture media until a specific time point. The cell culture media was changed every 3 days.

2.5.3. Live/dead staining

Live and dead cell images were observed under a Super Resolution Confocal Laser Scanning Microscope (LSM 880 with Airyscan, Carl Zeiss, Germany) with the process of Z-stack. A live/dead cell imaging kit (Invitrogen, CA, USA) was used for the staining. To prepare the live and dead staining reagent, a calcein-AM (green) was added to an Ethidium homodimer (red). The cell encapsulated scaffolds were cultured for 3, 14 days and were placed on a confocal dish (Cell Culture-Treated, STERILE, SPL Life Sciences Co., Ltd., South Korea). The reagent was added to the scaffolds and incubated in a 5% CO_2 and 37 ℃ cell culture incubator for 1 hr.

2.5.4. MTT assay

The viability of the cell-cultured scaffolds was evaluated by MTT assay on 1, 7, and 14 days of culture. The culture medium of the scaffolds was replaced with a 1 mL fresh medium and 100 μL of MTT solution (5 mg/mL in PBS) was added to the specimens. The samples were incubated in 5% of CO_2 and 37 ℃ cell culture incubator for 4 hrs. After incubation, the medium was removed and 1 mL of dimethyl sulfoxide (DMSO; Sigma-Aldrich, USA) was added. 100 μL of the solubilized solution was transferred to a 96-well plate and measured with a microplate reader (Emax Molecular Devices, CA, USA) at 570 nm.

2.5.5. Real-time polymerase chain reaction

Cell lysis was performed by adding a Trizol (Invitrogen, USA) to the cell-cultured scaffolds and was pipetted. The specimens were placed in an EP tube (Eppendorf, USA) and chloroform (SAMCHUN chemicals, South Korea) was added. The solution was shaken homogeneously and was centrifuged at 12000 rpm at 4 ℃ for 15 min. The supernatant was transferred to a new 1.5 mL EP tube and 0.5 mL of ice-cold isopropanol (Sigma-Aldrich, USA) was added. The specimens were stored at -20 ℃ overnight. Then, the samples were centrifuged at 12000 rpm at 4 ℃ for 15 min and the supernatant was removed. 0.5 mL of 75% ethanol was added to the samples to wash and centrifuged at 7000 rpm at 4 ℃ for 5 min. The ethanol was removed and stored at room temperature to fully dry the tube. The extracted mRNA was diluted with 40 μL of RNase-DNase-free water (Gibco, USA). The mRNA concentration was measured with a Biospectrophotometer (Eppendorf, USA). A TOPscriptTM RT DryMIX (dT18 plus) (Enzynomics, South Korea) and a PCR Thermal cycler (Takara, Japan) were used to synthesize cDNA. The cDNA was kept at -20 ℃ overnight and the concentration was measured once again. SYBR™ Green PCR Master Mix (Applied Biosystems, USA), specific genes and samples were mixed to evaluate real-time PCR using StepOnePlus Real-Time PCR system (Applied Biosystems, USA). The alkaline phosphatase (ALP), collagen type 1 (COL1), osteocalcin (OCN), and runt-related transcription factor 2 (RUNX-2) were used for the study and glyceraldehyde 3-phosphate dehydrogenase (GAPDH) was used as a housekeeping gene. The gene expression was calculated according to an equation of $2^{-\Delta\Delta CT}$.[30] The gene sequences of the primers are listed in Table 2.

Table 2. Primer sequences for quantitative RT-PCR

Protein		Primer sequence
GAPDH	Forward	5′ GGC ACA GTC AAG GCT GAG AAT G 3′
	Reverse	5′ ATG GTG GTG AAG ACG CCA GTA 3′
ALP	Forward	5′ GAC ATC GCC TAC CAG CTC AT 3′
	Reverse	5′ TCA CGT TGT TCC TGT TCA GC 3′
COL1	Forward	5′ CTG ACT GGA AGA GCG GAG AGT AC 3′
	Reverse	5′ CCA TGT CGC AGA AGA CCT TGA 3′
OCN	Forward	5′ AGA GTC TGG CAG AGG CTC A 3′
	Reverse	5′ CAC TGT TGA AGT CGC AGG AG 3′
RUNX2	Forward	5′ CCC TGA ACT CTG CAC CAA GT 3′
	Reverse	5′ GTG CCT CGT GTG GAA GAC A 3′

3. Results and discussion

3.1. Morphology and biological activity characterization

In this study, we fabricated the designed scaffolds in the way (Figure 1). The morphology and formation of HA were charac-

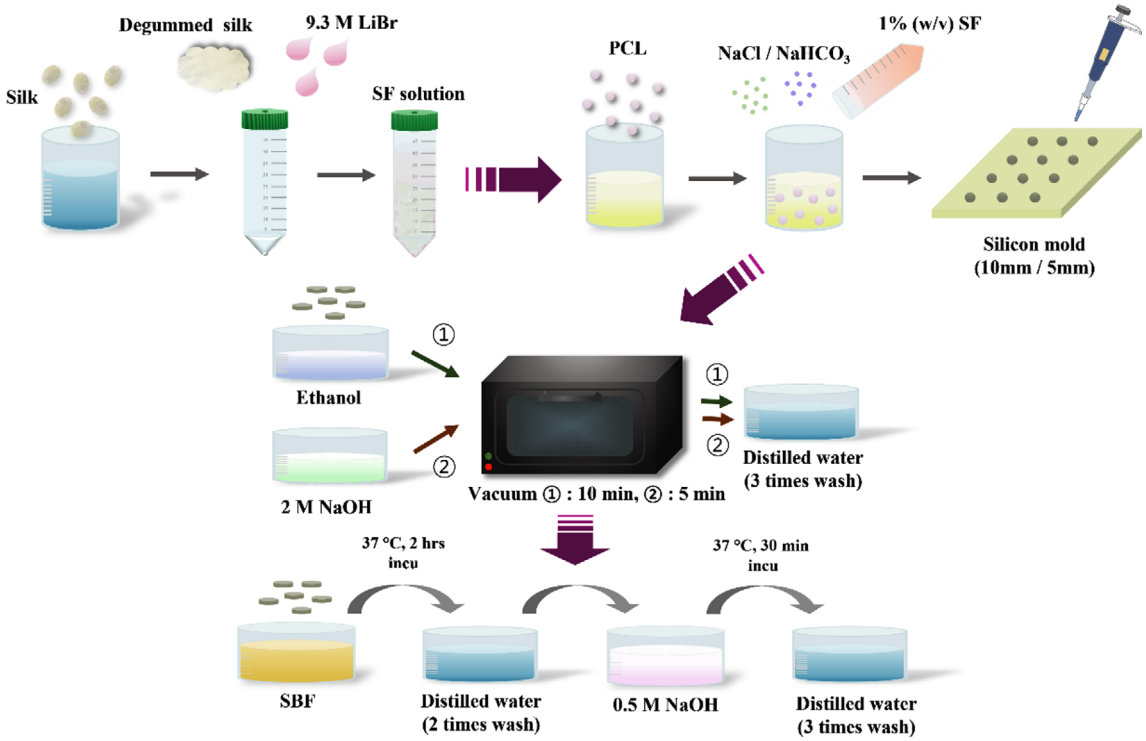

Figure 1. Summary of the work was presented as scheme.

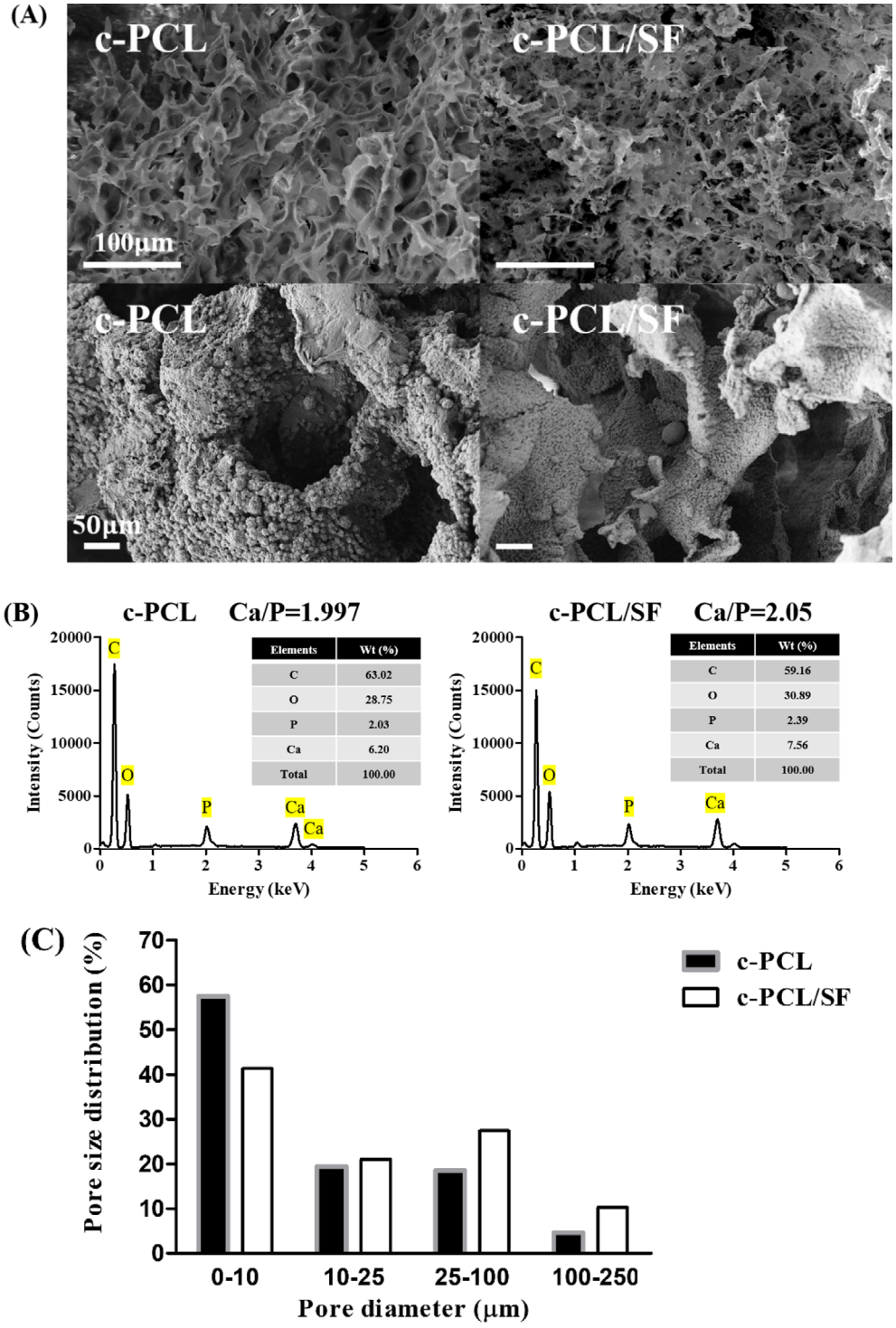

Figure 2. (A) Morphological study, (B) EDS micrographs, and (C) pore size distribution (%) of the coated PCL and PCL/SF scaffolds.

terized by SEM, FE-SEM, and EDS. The SEM images of the c-PCL and c-PCL/SF scaffolds are shown in Figure 2(A). The pore size of the scaffolds was measured by ImageJ software (Figure 2(C)). The average large pore sizes of ~225 μm, medium pores of ~18 μm, and the small pores of ~6 μm were observed in c-PCL scaffolds, respectively. The pore sizes of c-PCL/SF scaffolds were ~210 μm, ~20 μm, and ~5 μm, respectively. The macropores are created by the salt leaching and gas foaming process and microporous structures are formed by the N-TIPS technique. The pore size of 100-200 μm helps eliminate bacteria and enhances the infiltration of cells. Also, a pore size of <10 μm induces ion exchange and protein adsorption. Lim et al. The larger the pore size, the more oxygen and nutrients are supplied, which promotes the formation of blood vessels so that more mature bones can be formed. However, a pore size in the range of 200-350 μm is most optimal for osteoblast proliferation, and a larger pore size may inhibit cell adhesion.[31] Therefore, the fabricated scaffolds are appropriate for bone tissue engineer-

ing. In particular, PCL/SF scaffold is expected to be more useful for cell infiltration and proliferation because it has a larger pore size of 100 to 250 μm (Figure 2(C)). The formation of HA was observed by FE-SEM (Figure 2(A)). Based on EDS analysis, the Ca/P ratio of the c-PCL scaffolds was 1.997 and the Ca/P ratio of the c-PCL/SF scaffolds was 2.05 (Figure 2(B)). EDS analysis shows increased Ca concentration with calcination temperature treatment. When the $CaCO_3$ compound is heated, it decomposes into CaO and CO_2. As the Ca/P ratio increases, the porosity (%) of the calcium phosphate matrix tends to decrease. According to the results of previous experiments, the higher the Ca/P ratio, the greater the adhesion of osteoblasts to calcium phosphate. Both c-PCL and c-PCL/SF scaffolds have a Ca/P ratio close to 2, but at a ratio of 2.0, the presence of CaO can reduce the viability of osteoblasts, so the ratio needs to be adjusted.[32,33] That indicates a molar ratio of the c-PCL/SF is higher than PCL scaffolds which may be due to the strong interaction between Ca^{2+} and carboxy groups of SF.[21]

3.2. Physicochemical and mechanical properties

The porosity, mass swelling, and weight loss over time were measured (Figure 3). High porosity increases the cell growth, migration, and adhesion of the scaffold.[34] In addition, a higher degree of porosity increases the surface area which allows more CaP coating and adsorption of protein.[35] The c-PCL and c-PCL/SF scaffolds showed a porosity of ~75% and ~80%, respectively. (Figure 3(A)). One of the forms of bone tissue is a trabecular bone which provides a porous environment with a porosity of 50-90%.[36] That indicates the fabricated scaffolds have sufficient value of porosity for bone tissue engineering. The mass swelling of the scaffolds showed 65±4% and 67±4% in c-PCL and c-PCL/SF, respectively (Figure 3(B)). The difference did not show among the scaffolds which may be due to the similar porosity of the c-PCL and c-PCL/SF scaffolds. The weight loss analysis of the scaffolds was performed for 28 days (Figure 3(C)). At the initial time point, the weights of all samples increased due to the water permeation. After 7 days of the study, weights of the scaffolds were decreased, and degradation occurred. On 28 days of weight loss analysis, coated PCL scaffolds showed a weight loss of ~4%, and coated PCL/SF scaffolds showed a weight loss of ~6% which did not show a significant difference. PCL was expected to have a difference in swelling and decomposition behavior because the surface is less hydrophilic due to the non-polar methylene group and SF is a material with hydrophilicity, but there was no significant difference. Both groups showed slow degradation, which is advantageous in terms of structural stability.[37] This result indicates that the incorporation of SF does not hinder the property of PCL. The mechanical properties of the scaffolds were measured by compression test. The compressive strength value of c-PCL/SF was significantly higher when compared to the c-PCL scaffold (Figure 3(D)). The compressive modulus at the strain of 5-10% was calculated as ~97 kPa and ~143 kPa in c-PCL and c-PCL/SF scaffolds. This may be due to the composition of β-sheet crystals of SF formed by hydrogen bonds between hydrophobic crystalline regions of heavy chain and amorphous domains.[16,38] The main constituent of the crystal region is a polypeptide chain mainly composed of the amino acids glycine (Gly) and alanine (Ala), and adjacent chains are joined by strong hydrogen bonds in an antiparallel arrangement to

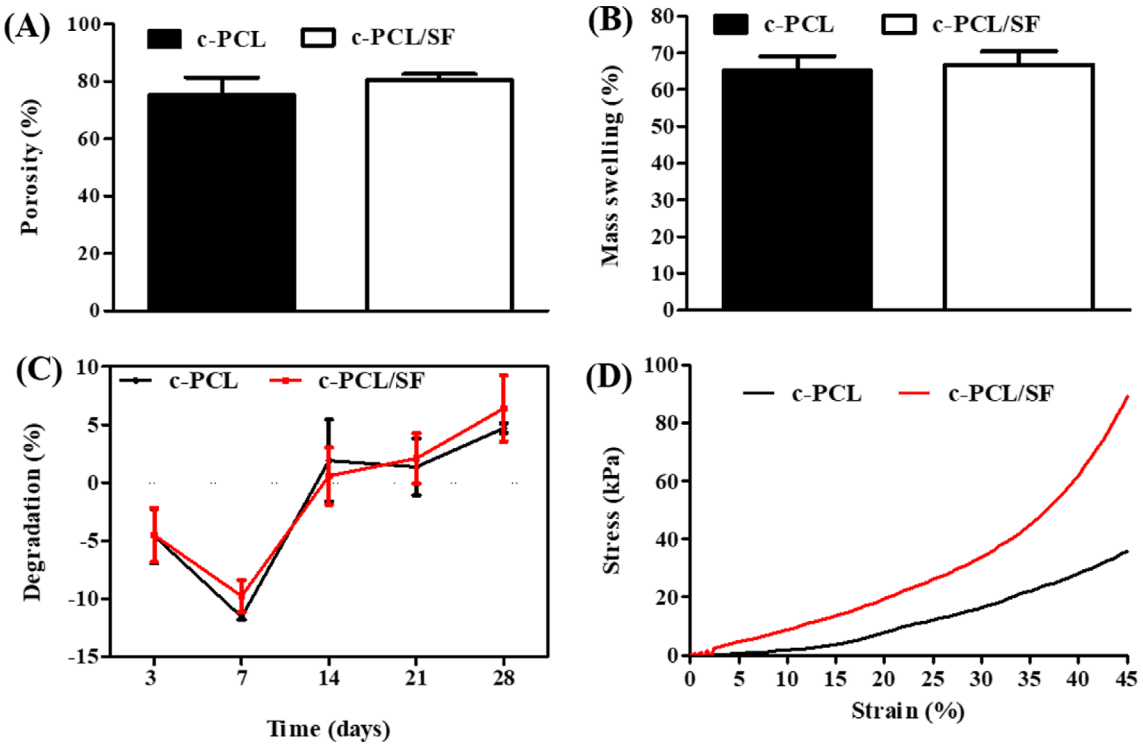

Figure 3. Physicochemical and mechanical study of the fabricated scaffolds: (A) porosity (%), (B) mass swelling (%), (C) weight loss study, and (D) stress-strain curve of the coated PCL and PCL/SF scaffolds (values are mean±SD (N=4), $P < 0.01$ (**) and $P < 0.001$ (***)).

form a B-sheet. Due to this strong interaction, the c-PCL/SF scaffold has a higher mechanical strength.[38] The compressive modulus of 10 wt% pure PCL scaffolds was increased compared to the previous study which indicated the methods that we used in this study such as biomimetic calcium phosphate coating, N-TIPS, salt leaching, and gas foaming was more favorable for biomaterials.[39]

3.3. *In vitro* analysis

To evaluate the viability of cells and cytotoxicity of the scaffolds, an MTT assay was performed on 3, 7, and 14 days of culture (Figure 4(A)). All samples showed no significant difference in cell growth for 14 days. Cells showed rapid proliferation after 7 days of culture. This result indicates the incorporation of SF in PCL does not harm the biocompatibility of the scaffolds. Furthermore, the viability and growth of cells were characterized by live/dead staining (Figure 4(B)). On 3 days of culture, only a few of dead cells was observed in both coated PCL and PCL/SF groups. After 3 days of cell culture, there was no significant difference in the viability of the rBMSCs in both groups. This result indicates no harmful effect of the scaffolds. On 7 and 14 days of culture, c-PCL/SF showed an increase in the cell number and a significantly highest intensity as a result of the live staining

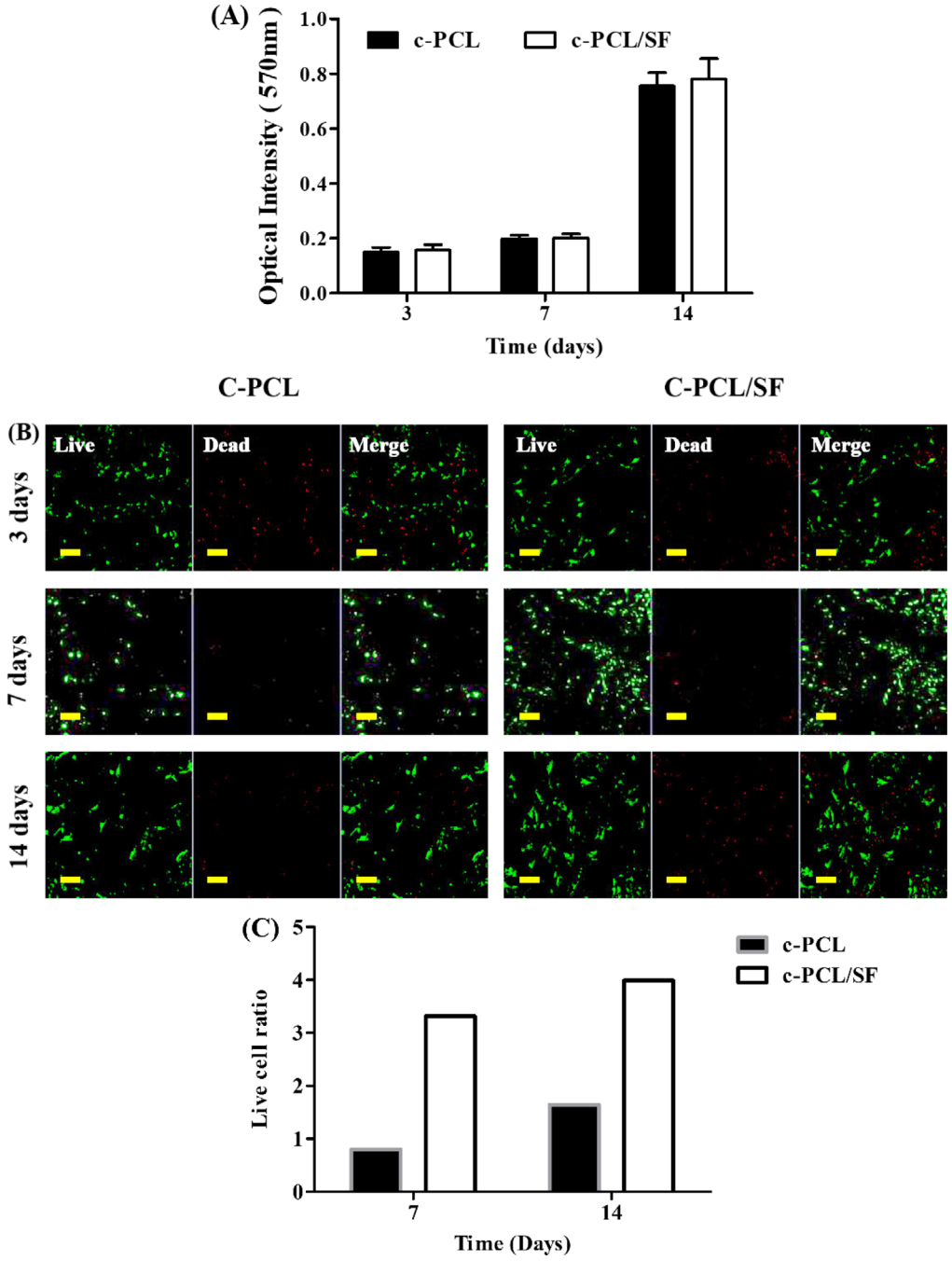

Figure 4. Cell viability; (A) MTT assay of BMSC-laden scaffolds for 3, 7, 14 days, (B) Live & Dead stain micrographs of PCL, and PCL/SF scaffolds magnification 100 × with 3 and 7 days of PCL, PCL/SF scaffolds (scale bar=100 μm), and (C) Live cell ratio for 7 and 14 days relative to 3 days (values are mean±SD (N=4), $P < 0.01$ (**) and $P < 0.001$ (***)).

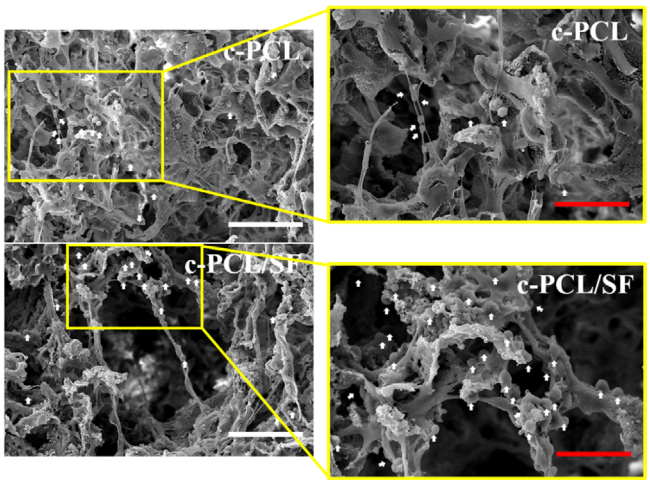

Figure 5. Morphology of the cells cultured in PCL and PCL/SF scaffolds for 14 days (100 μm for white scale bar and 50 μm for red scale bar).

(Figure 4(C)). The enhancement of cell growth and proliferation in the PCL/SF group is due to the favorable microenvironment of the SF. The hydrophilicity of SF from amide (-CONH) and hydroxyl (-OH) groups induce growth and attachment of the cells on the surface of the scaffolds. Hydrophilicity enhances surface energy which promotes cell adhesion, differentiation, and proliferation.[15] On 14 days of culture, round cells changed to elongated and spindle-shaped cells. This result indicates the cell adherence properties and interaction between cells and scaffolds in the c-PCL/SF scaffolds were improved.[40] rBMSCs were cultured for 14 days on the scaffolds to characterize the morphology of cells (Figure 5). On 14 days of culture, the cells were dispersed uniformly in the porous structure. The coated PCL/SF scaffolds showed a prominent intercellular extracellular matrix (ECM) which indicates enhanced cell-cell and cell-matrix interaction.[41] Osteogenic differentiation of the c-PCL and c-PCL/SF scaffolds were characterized by real-time polymerase chain reaction (RT-PCR) after 3 and 14 days of culture (Figure 6). The bone-specific genes such as ALP, COL1, RUNX2, OCN were used for the analysis. GAPDH housekeeping gene was used for normalization. ALP is an important marker of bone formation differentiation. COL1 is involved in ECM formation and a large amount of COL1 is observed during proliferation.[42] OCN is a noncollagenous protein secreted by osteoblasts and possesses many Ca^{2+} binding domains.[43,44] RUNX2 regulates osteogenic differentiation and is an essential transcription factor to express specific genes such as ALP, COL1, and OCN.[45] The values of ALP, COL1, OCN, and RUNX2 showed higher expressions on the c-PCL/SF scaffolds due to the higher compressive strength of the c-PCL/SF scaffolds. This result shows the osteogenic differentiation was induced. The osteogenic differentiation can be promoted by the rigidity of the scaffolds.[46,47] Commonly, ALP activity is an indicator of immature osteoblast activity. Moreover, it has been described that ALP cleavage of organic phosphate plays a role in the mineralization of the extracellular collagenous matrix by providing calcium and phosphate ions to generate new formation of the cell-mediated calcium phosphate mineralized matrix.[48] Figure 7 shows the course of ALP activities of cultured BMSCs on each scaffold after 3 and 14 days. ALP activity of c-PCL was 46±0.2 and 53±0.3 (ng*mg ($^{-1}$)) for 3 and 14 days, respectively. And ALP activity of c-PCL/SF was 49±0.1 and 57±0.5 (ng*mg ($^{-1}$)) for 3 and 14 days, respectively. Both c-PCL and c-PCL/SF scaffold showed an increase of the ALP activity for 3 and 14 days.

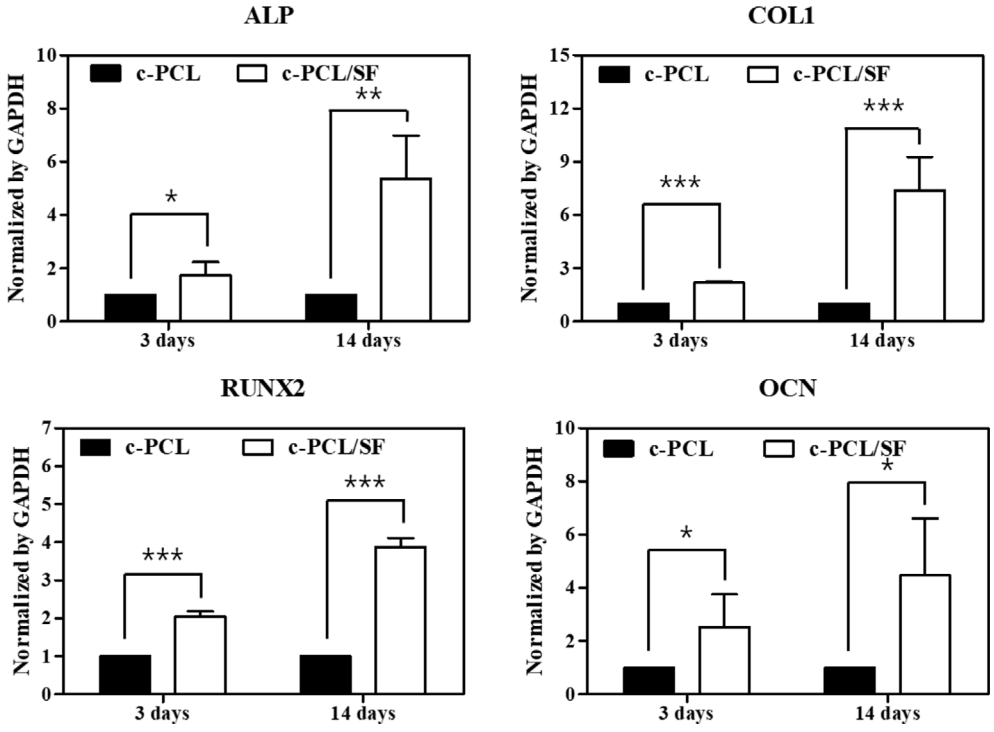

Figure 6. mRNA expression of bone-specific genes. (A) Alkaline phosphatase (ALP), (B) collagen type 1 (COL1), (C) runt-related transcription factor 2 (RUNX-2), and (D) osteocalcin (OCN) of BMSCs cultured on PCL, PCL/SF scaffolds analyzed on 3 and 14 days normalized by GAPDH (values are mean±SD (n=4), $P < 0.05$ (*), $P < 0.005$ (*), and $P < 0.0001$ (***)).

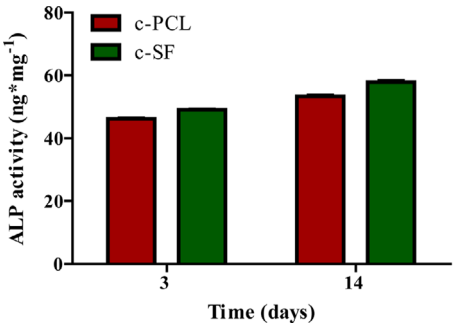

Figure 7. ALP activity (ng*mg^(-1)) of PCL and PCL/SF scaffolds analyzed on 3 and 14 days of culture.

There is an insignificant difference, but ALP activity of coated PCL/SF scaffold is slightly higher on two days. Overall result confirms that c-PCL/SF scaffold has a positive effect on the osteoinductive property and osteogenic differentiation for bone tissue engineering.

4. Conclusion

In this study, we show the difference in the bone regeneration effect of biomimetic coated PCL scaffolds with and without SF and evaluate their effect on proliferation, adhesion and differentiation of RBMSCs. Numerous studies have developed PCL scaffolds for bone regeneration and enhancement of bone formation. SF was incorporated in PCL and the scaffolds were fabricated by salt leaching, gas foaming, and N-TIPS method to form macro- and microporous structures. The microenvironment and bioactivity of the scaffolds were enhanced by biomimetic calcium phosphate coating. The characterization and *in vitro* studies were carried out. The biological activity evaluated by FE-SEM and EDS analysis showed the higher formation of apatite in the PCL/SF scaffolds. The physicochemical properties of the scaffolds did not show a significant difference among c-PCL and c-PCL/SF scaffolds but the c-PCL/SF scaffold had slightly higher porosity, swelling degree and degradation rate, indicating that the incorporation of SF was not significantly different from that of PCL. This implies that the incorporation of SF does not harm the property of PCL. However, the mechanical property improved in c-PCL/SF scaffolds. The biocompatibility of the scaffolds did not show a significant difference, but the bioactivity was enhanced in the c-PCL/SF. This is due to the β-sheet structure of SF formed by hydrogen bonding between the hydrophobic crystalline region and the amorphous region of the chain. Because of the hydrophilicity of SF, the PCL/SF scaffold induced cell growth and adhesion to the scaffold surface and showed many cell proliferation and differentiation. The c-PCL/SF scaffolds showed higher expression of bone-specific genes and this result shows that the incorporation of SF improves the osteoinductive property and osteogenic differentiation. In conclusion, our studies suggest that c-PCL/SF scaffold is a promising scaffold for bone tissue engineering because of its bioactivity, biocompatibility, mechanical property, enhanced surface property, and microenvironment for cell adhesion, proliferation, differentiation.

Conflicts of interest: The authors declare no conflict of interest.

References

(1) S. Ragunathan, G. Govindasamy, D. R. Raghul, M. Karuppaswamy, and R. K. VijayachandraTogo, *Mater. Today Proc.*, **2**3, 111 (2019).
(2) L. Xiao, M. Wu, F. Yan, Y. Xie, Z. Liu, H. Huang, Z. Yang, S. Yao, and L. Cai, *Int. J. Biol. Macromol.,* **172**, 19 (2021).
(3) X. Xing, G. Cheng, C. Yin, X. Cheng, Y. Cheng, Y. Ni, X. Zhou, H. Deng, and Z. Li, *Arab. J. Chem.*, **13**, 5526 (2020).
(4) M. Farokhi, F. Mottaghitalab, S. Samani, M. A. Shokrgozar, S. C. Kundu, R. L. Reis, Y. Fatahi, and D. L. Kaplan, *Biotechnol. Adv.*, **36**, 68 (2018).
(5) R. Dwivedi, S. Kumar, R. Pandey, A. Mahajan, E. Nandana, D. S. Katti, and D. Mehrotra, *J. Oral Biol. Craniofacial Res.*, **10**, 381 (2020).
(6) J. Luo, H. Zhang, J. Zhu, X. Cui, J. Gao, X. Wang, and J. Xiong, *Colloids Surf. B Biointerfaces*, **163**, 369 (2018).
(7) A. A. Ia and A. A. Kareem, *Mater. Sci. Pol.*, **34**, 132 (2016).
(8) M. Abedalwafa, F. Wang, L. Wang, and C. Li., *Rev. Adv. Mater. Sci.*, **34**, 123 (2013).
(9) M. A. Nazeer, E. Yilgor, and I. Yilgor, *Polymer*, **168**, 86 (2019).
(10) S. R. Caliari and J. A. Burdick, *Nat. Methods*, **13**, 405 (2016).
(11) A. A. Kareem, *Mater. Sci. Pol.*, **35**, 755 (2017).
(12) A. A. Kareem, *Mater. Sci. Pol.*, **36**, 283 (2018).
(13) A. A. Kareem, *Adv. Compos. Lett.*, **29**, 1 (2020).
(14) H. K. Rasheed, and A. A. Kareem, *J. Opt. Commun.*, **42**, 25 (2021).
(15) S. Inoue, K. Tanaka, F. Arisaka, S. Kimura, K. Ohtomo, and S. Mizuno, *J. Biol. Chem.*, **275**, 40517 (2000).
(16) N. Drnovšek, R. Kocen, A. Gantar, M. Drobnič-Košorok, A. Leonardi, I. Križaj, A. Rečnik, and S. Novak, *J. Mater. Chem. B*, **4**, 6597 (2016).
(17) H. K. Rasheed, and A. A. Kareem, *Iraqi. J. Sci.*, **61**, 3235 (2020).
(18) X. D Kong, F. Z. Cui, X. M. Wang, M. Zhang, and W. Zhang, *J. Cryst. Growth*, **270**, 197 (2004).
(19) Y. Meng, Y. X. Qin, E. Dimasi, X. Ba, M. Rafailovich, and N. Pernodet, *Tissue Eng. Part A*, **15**, 355 (2009).
(20) J. Jeong, J. H. Kim, J. H. Shim, N. S. Hwang, and C. Y. Heo, *Biomater. Res.*, **23**, 1 (2019).
(21) Q. Hu, Z. Tan, Y. Liu, Jinhui Tao a, Y. Cai, M. Zhang, H. Pan, X. Xu, and R. Tang, *J. Mater. Chem.*, **17**, 4690 (2007).
(22) A. A. Kareem and H. K. Rasheed, *Mater. Sci. Pol.*, **37**, 622 (2019).
(23) A. A. Kareem, H. K. Rasheed, and E. M. Nasir, *Polym. Bull.*, **79**, 6617 (2021).
(24) H. Zhang, X. Liu, M. Yang, and L. Zhu, *Mater. Sci. Eng. C*, **55**, 8 (2015).
(25) J. T. Jung, H. H. Wang, J. F. Kim, J. Lee, J. S. Kim, E. Drioli, and Y. M. Lee, *J. Membr. Sci.*, **559**, 117 (2018).
(26) V. Cannillo, F. Chiellini, P. Fabbri, and A. Sola, *Compos. Struct.*, **92**, 1823 (2010).
(27) D. Y. Kwon, J. Y. Park, B. Y. Lee, and M. S. Kim, *Polymers*, **12**, 2210 (2020).
(28) F. Dehghani, and N. Annabi, *Curr. Opin. Biotechnol.*, **22**, 661 (2011).
(29) F. Yang, J. G. C. Wolke, and J. A. Jansen, *Chem. Eng. J.*, **137**, 154 (2008).
(30) K. J. Livak and T. D. Schmittgen, *Methods*, **25**, 402 (2001).
(31) N. Abbasi, S. Hamlet, R. M. Love, and N. T. Nguyen, *J. Sci. Adv. Mater. Devices*, **5**, 1 (2020).
(32) M. Sari, P. Hening, Chotimah, I. D. Ana, and Y. Yusuf, *Biomater. Res.*, **25**, 1 (2021).
(33) H. Liu, H. Yazici, C. Ergun, T. J. Webster, and H. Bermek, *Acta Biomater.*, **4**, 1472 (2008).
(34) S. Zeng, L. Liu, Y. Shi, J. Qiu, W. Fang, M. Rong, Z. Guo, and W. Gao, *PLoS One*, **10**, 1 (2015).
(35) K. Wang, C. Zhou, Y. Hong, and X. Zhang, *Interface Focus*, **2**, 259 (2012).
(36) T. Almela, I. M. Brook, K. Khoshroo, M. Rasoulianboroujeni, F. Fahimipour, M. Tahriri, E. Dashtimoghadam, A. El-Awa, L. Tayebi, and K. Moharamzadeh, *Bioprinting*, **6**, 1 (2017).

(37) X. Liu, B. Chen, Y. Li, Y. Kong, M. Gao, L. Z. Zhang, and N. Gu, *J. Bioact. Compat. Polym.*, **36**, 59 (2021).
(38) Y. Cheng, L. D. Koh, D. Li, B. Ji, M. Y. Han, and Y. W. Zhang, *J. R. Soc. Interface*, **11** (2014).
(39) M. Yeo and G. Kim, *J. Mater. Chem. B*, **2**, 314 (2014).
(40) O. Jung, M. Radenkovic, S. Stojanovic, C. Lindner, M. Batinic, O. Görke, J. Pissarek, A. Pröhl, S. Najman and M. Barbeck, *In Vivo (Brooklyn)*, **34**, 2287 (2020).
(41) J. H. Choi, D. K. Kim, J. E. Song, J. M. Oliveira, R. L. Reis, and G. Khang, *Adv. Exp. Med. Biol.*, **1077**, 371 (2018).
(42) X. Ying, X. Chen, H. Liu, P. Nie, X. Shui, Y. Shen, K. Yu, and S. Cheng, *Eur. J. Pharmacol.*, **765**, 394 (2015).
(43) J. K. Burkhardt, D. Halama, B. Frerich, and F. Gaunitz, *Anal. Bioanal. Chem.*, **393**, 1351 (2009).
(44) J. T. Huh, J. U. Lee, W. J. Kim, M. Yeo, and G. H. Kim, *Int. J. Biol. Macromol.*, **110**, 488 (2018).
(45) S. Saravanan, A. Chawla, M. Vairamani, T. P. Sastry, K. S. Subramanian, and N. Selvamurugan, *Int. J. Biol. Macromol.*, **104**, 1975 (2017).
(46) M. Z. Witkowska, K. Walenko, E. Wrobel, P. Mrowka, A. Mikulska, and J. Przybylski, *Cell Biol. Int.*, **37**, 608 (2013).
(47) E. Ko, J. S. Lee, H. Kim, S. Y. Yang, D. Yang, K. Yang, J. Y. Lee, J. Shin, H. S. Yang, W. H. Ryu, and S. W. Cho, *ACS Appl. Mater. Interfaces*, **10**, 7614 (2018).
(48) J. B. Lee, J. E. Kim, M. S. Bae, S. A. Park, ,D. A. Balikov, H. J. Sung, H. B. Jeon, H. K. Park, S. H. Um, K. S. Lee, and I. K. Kwon, *Polymers (Basel)*, **8**, 1 (2016).

